lncRNA HOTAIR overexpression promotes hybrid epithelial/mesenchymal phenotype through suppression of c-Met Receptor Tyrosine Kinase Signaling in Hepatocellular Carcinoma Cells

Hande Topel
Syddansk Universitet https://orcid.org/0000-0001-5743-4019
Ezgi Bagirsakci
Izmir Biomedicine and Genome Center
Dehan Comez
Izmir Biomedicine and Genome Center
Gulsun Bagci
Izmir Biomedicine and Genome Center
Gulcin Cakan-Akdogan
Izmir Biomedicine and Genome Center
Nese Atabey (nese.atabey@ibg.edu.tr)
https://orcid.org/0000-0003-4966-2980

Research

Keywords: HCC, long non-coding RNA, HOTAIR, c-Met, Caveolin-1, hybrid E/M

Posted Date: February 11th, 2020

DOI: https://doi.org/10.21203/rs.2.23211/v1

Version of Record: A version of this preprint was published on July 11th, 2020. See the published version at https://doi.org/10.1186/s12964-020-00602-0.

Abstract

Background: Epithelial-to-mesenchymal transition (EMT) and mesenchymal-to-epithelial transition (MET) are both reversible processes, and regulation of phenotypical transition is very important for progression of several cancers including hepatocellular carcinoma (HCC). Recently, it is defined that cancer cells can attain a hybrid epithelial/mesenchymal (hybrid E/M) phenotype. Cells with hybrid E/M phenotype comprise mixed epithelial and mesenchymal properties, they can be more resistant to therapeutics and also more capable of initiating metastatic lesions. However, the mechanisms regulating hybrid E/M in HCC are not well described yet. In this study, we investigated the role of the potential crosstalk between lncRNA HOTAIR and c-Met receptor tyrosine kinase, which are two essential regulators of EMT and MET, in acquiring of hybrid E/M phenotype in HCC.

Methods: Expression of c-Met and HOTAIR were defined in HCC cell lines and patient tissues through HCC progression. lncRNA HOTAIR was overexpressed in SNU-449 cells and its effects on c-Met signaling were analyzed. c-Met was overexpressed in SNU-398 cells and its effect on HOTAIR expression was analyzed. Biological significance of HOTAIR/c-Met interplay was defined in means of adhesion, proliferation, motility behavior, invasion, spheroid formation and metastatic ability. Effect of ectopic HOTAIR expression on phenotype was defined with investigation of molecular epithelial and mesenchymal traits.

Results: In vitro and in vivo experiments verified the pivotal role of lncRNA HOTAIR in acquisition of hybrid E/M phenotype through modulating c-Met and its membrane co-localizing partner Caveolin-1 expression, activation and membrane organization to cope with the rate limiting steps of metastasis such as survival in adhesion independent microenvironment, escaping from anoikis and resisting to fluidic shear stress (FSS) in HCC.

Conclusions: Our work provides the first evidence suggesting a role for lncRNA HOTAIR in the modulation of c-Met to promote hybrid E/M phenotype. The balance between lncRNA HOTAIR and c-Met might be critical for cell fate decision and metastatic potential of HCC cells.

Background

Liver cancer is ranked as 7th cancer type in the list of cancers with the highest number of cases incident between 2007 and 2017 by Global Burden of Disease (GBD) 2017 study. Hepatocellular Carcinoma (HCC) accounts more than 80% of liver cancer cases and it is estimated to be the 4th most common cause of cancer related deaths worldwide (1). HCC is reported to have complex and heterogeneous molecular features which is previously stressed out by integrative studies combining genomic characterization, exome sequencing, transcriptome analysis and clinical trials. Molecular heterogeneity and etiological complexity of HCC makes it unlikely for one treatment or agent to effectively target all or most HCCs (2, 3).

c-Met, a receptor tyrosine kinase, is known to be upregulated in liver diseases favoring hepatocyte proliferation. Besides potential benefits in chronic liver diseases, c-Met contributes to initiation,

development and progression of HCC. c-Met activation in HCC is mostly driven by molecular networks instead of activating mutations and it is activated by non-canonical signaling mechanisms as well as canonical activation by its ligand, HGF. c-Met is regarded as one of the most promising targets for HCC treatment and c-Met targeted clinical trials are being conducted, currently (4). In addition to its contribution to HCC development and progression, c-Met is also considered to be a key player in drug resistance (5).

HOX transcript antisense intergenic RNA, HOTAIR, is a 2,148-nt-long spliced and polyadenylated long non-coding RNA (lncRNA) encoded within HOXC cluster. HOTAIR is first defined to take role in epidermal tissue development by recruiting chromatin remodeling complexes to its epigenetic targets (6, 7). Overexpression of HOTAIR has been associated with poor prognosis, invasiveness and aggressiveness of various cancer types (8–11). Complex secondary structure and ability to form independent structural domains ensure the multi-acting nature of HOTAIR and it has been defined to contribute to various cellular mechanisms via different molecular interactions such as scaffolding protein complexes, decoying microRNAs, epigenetically targeting genes and enabling RNA-protein/DNA-protein interactions (7, 12–14).

Transcription factors, non-coding RNAs and epigenetic regulators play critical roles in cell-fate determination such as transition between epithelial and mesenchymal phenotypes. Starting from the origin of a tumor, cancer cells go through complex and dynamic phenotypical changes -epithelial to mesenchymal transition (EMT), or its reverse mesenchymal to epithelial transition (MET)- to cope with metastasis rate-limiting steps. It has been reported that, some cancer cells display both epithelial and mesenchymal markers and this phenotype referred as hybrid, intermediate, partial, metastable or incomplete EMT phenotype (15–18). The tumor cells simultaneously expressing both mesenchymal and epithelial markers may be more plastic and most likely to contribute to metastatic outgrowth. Cells bearing this hybrid phenotype are first defined in circulating tumor cells (CTCs) of patients with both epithelial and mesenchymal traits (19, 20). Hybrid cells that co-express mesenchymal and epithelial markers migrate collectively, more resistant to fluidic shear stress damage in circulation, exit from anoikis and have enhanced metastatic ability than cells with complete epithelial or mesenchymal phenotypes (21). That is why, cancer cells that attain a hybrid E/M (epithelial/mesenchymal) phenotype pose greater risk for metastasis in cancer patients (22).

c-Met is reported to play an essential and complex role in modulation of transitional states within the broad spectrum of cellular phenotypes (23). Although HOTAIR is also reported to contribute attainment of cellular phenotypes, its role is generally defined in means of correlations with aggressiveness traits of cancer cells (10, 11, 24, 25). As the number of the studies reporting induced expression and critical roles of these two molecules in HCC are increasing, the likelihood of their direct or indirect molecular interaction becomes non-negligible. In this study, we aimed to investigate the nature of their interaction and here, we describe the interplay between HOTAIR and c-Met in HCC context. Our data present strong evidence that HOTAIR ensures hybrid E/M phenotype and its downregulation is required for c-Met induced complete mesenchymal phenotype in HCC cells.

Materials And Methods

Cell Culture

All Human HCC cell lines were kindly provided by Prof. Dr. Mehmet Öztürk (Izmir Biomedicine and Genome Center, Izmir, Turkey). FOCUS, SNU-449, SK-HEP-1, SNU-475, SNU-387, SNU-423, SNU-398, MAHLAVU, HEP-3B and HuH-7 cell lines were cultured as described previously (26). All cell lines were tested for mycoplasma infection and confirmed as negative before the experiments. SU11274 (Calbiochem, 448101) solubilized with DMSO used with 2500 nM concentration. c-Met kinase activity was inhibited with SU11274 (2500 nM in 2% FBS complete medium). Ligand dependent c-Met activation was induced by 10 ng/ml Hepatocyte Growth Factor (HGF) in 2% FBS complete medium (R&D system, USA). Sorafenib treatment was continuously applied with the amount of their growth inhibition 50 (GI50) values (6 µM of Sorafenib) to Mahlavu sorafenib resistant cell clones which have been established in our previous studies (5).

Cells were sheared with 205 U/CA multichannel peristaltic pump and Marprene tube elements of 2.79 bore for tubing (Watson Marlow, UK). Adherent cells were detached with 0.25 % Trypsin /EDTA (Biological Industries, #03-050-1B, Israel) and 3 million cells in 8 ml of culture media were cultured in circulation under 0.5 dyn/ cm^2 shear stress at 37^oC, in humidified incubator supplied with 5% $CO_{2,}$ for one hour. After FSS application, cells were stained with trypan blue and counted with hemocytometer to evaluate cell viability under shear stress.

mRNA Isolation

NucleoSpin RNA Isolation kit (Macherey-Nagel, Germany) has been used for mRNA isolation. mRNA isolation performed according to the manufacturer's instructions. mRNA eluted with DNAse/RNAse free distilled water and its concentration is measured via NanoDrop.

Reverse Transcription and RT-qPCR

SensiFast^{TM} cDNA Synthesis Kit (Bioline Meridian Bioscience, USA) were used to transcribe cDNA from mRNA. qPCR reactions were performed with primers designed specific for cDNA sequences of gene of interests (CDS) from NCBI-Gene Bank. RT-qPCR analysis performed using SensiFast^{TM} SYBR No-ROX kit (Bioline Meridian Bioscience, USA) with ABI 7500 Fast Real-Time PCR System (Thermo Scientific, USA) according to the manufacturer's instructions. RPL41 and/or GAPDH gene expressions were used as internal control to normalize relative expression of the genes. Primers targeting mRNAs of interest were listed in Supplementary Document 1.

Fluorescent In-Situ Hybridization (FISH)

HOTAIR mRNA was hybridized with Stellaris® FISH Probes, Human HOTAIR with Quasar® 570 Dye (LGS Biosearch Technologies, VSMF-2178-5). HCC cells were grown on glass coverslips and fixed with 3:1 methanol-acetic acid (MeOH-AcOH) fixation solution for 10 minutes. Hybridization was performed

according to the manufacturer's instructions with 500 nM HOTAIR targeting probes for 4 hours at 37^{o}C. Cell nucleus was stained with DAPI.

Labeling with c-Met antibody and hybridizing HOTAIR mRNA with fluorescent-labeled probes were performed sequentially. For sequential labeling, HCC cells were firstly fixed with 3.7% (vol./vol.) formaldehyde in 1X-PBS for 10 minutes at room temperature. Fixed cells were incubated with primary antibody against c-Met protein (Cell Signaling, #3127) for 2 hours at room temperature. After couple of washes with 1X-PBS, cells were incubated with secondary antibody (Alexa488-conjugated goat anti-mouse secondary antibody, Invitrogen, A-11001) for 1 hour at RT. After immunofluorescent labeling, cells were fixed again with 3:1 methanol-acetic acid (MeOH-AcOH) fixation solution for 10 minutes. Following hybridization was performed according to the manufacturer's instructions with 500 nM HOTAIR targeting probes for 4 hours at 37^{o}C. Cell nucleus was stained with DAPI and cells were analyzed with Zeiss LSM 880-Confocal Laser Scanning Microscopy with Airyscan in IBG Optic Imaging Core Facility.

Immunoblotting

The cells were lysed using RIPA lysis buffer containing 1 mM Na3VO2, 1 mM NaF, and 1% protease inhibitor cocktail (Roche Diagnostics, Indianapolis, IN, USA), and the lysates were subjected to Western blot analysis as described previously (26). Primary antibodies are described in Supplementary Document 1.

Producing retroviral and lentiviral virus particles and generation of stable cell lines

SNU-449 cells were infected with retroviral vector bearing viruses. Retroviral vector bearing virus particles produced by transfection of HEK-293T cells with VSV-G envelope expressing plasmid (5µg), gag-pol expressing plasmid (5 µg) and retroviral target vectors (5 µg) together by Roche X-tremeGENE™ HP DNA Transfection Reagent (6366244001, Roche). After 24 hours of transfection, cell culture media refreshed and collected 48 hours post-transfection. HCC cells were infected with 1:1 titration of retrovirus containing media. After 48 hours, infected SNU-449 cells were selected with 13 µg/ml puromycine (Life Technologies, #A1113803, USA) for at least 3 passages.

HEK-293T cells were transfected with vectors bearing Rev (1 µg), gag-pol (6 µg) and VSV-G envelope (3 µg) proteins with lentiviral target vectors (2.5 µg) by transfection reagent. After 48 hours, cell culture media collected and SNU-398 cells were infected with 1:5 titration of lentivirus containing media. After 48 hours of infection, infected cells were selected with 2 µg/ml puromycine for at least 3 passages. Lentiviral and retroviral vectors and their origin are listed in Supplementary Document 1.

Immunofluorescent analysis of the cells

HCC cells were grown on glass cover-slips and after experimental conditions set, cells were immunofluorescently labeled as described in previous study (27). Imaging was performed with upright

fluorescence microscope (Olympus - BX61) and Zeiss LSM 880-Confocal Laser Scanning Microscopy with Airyscan at IBG Optic Imaging Core Facility.

Trans-well motility and invasion assays

Trans-well inserts with 8µm pore size (SPL Life Sciences, #37224, Korea) were used to analyze motility and invasion ability of HCC cells. The mix of 0.25 mg/ml basal membrane extract (Corning Matrigel® Growth Factor Reduced (GFR) Basement Membrane Matrix, Phenol Red-Free, #356231) was coated on invasion inserts. Trans-well motility and invasion experiments performed as described in previous study (26). Motile and invasive cells located at the exterior surface of the inserts were counted with bright field inverted microscope and statistical analysis was performed via Prism 8.

Real-time adhesion, proliferation, motility and invasion assays

Real-time cell growth monitoring was performed with the Real-Time Cell Analyzer, xCELLigence System (Roche, Germany) as described previously (28). 5000 cell/well was plated to analyze proliferation and adhesion to cell-culture treated wells of E-Plates. For motility and invasion assays, CIM-plates (ACEA Biosciences, # 0566581701, USA) were used with xCELLigence System. CIM-plate wells were coated with 0.25 mg/ml basal membrane extract (Corning Matrigel® Growth Factor Reduced (GFR) Basement Membrane Matrix, Phenol Red-Free, #356231) for invasion assay. For motility and invasion assays, 30.000 cells/well were plated to CIM-Plate wells and incubated for 24 hours by monitoring with xCELLigence RTCA system.

Hanging Drop Spheroid Formation Assay

The lid of 10 cm of tissue culture dish was inverted and 20µl medium-cell mix was placed on the inverted lid of dish results in formation of hanging-drop which contains 2.500 SNU-449 HOTAIR OE and SNU-449 MOCK cells per drop. The reservoir part of 10 cm of tissue culture dish was filled with 3-5 ml of 1X PBS to provide a humidified environment. The culture dish was incubated at 37^{o}C, 5% CO2, 95% humidified incubator for 72h or 96h until the spheroids formation and spheroids were imaged under Zeiss Stemi 508 stereo microscope.

2D Colony Formation Assay

SNU-449 HOTAIR OE and SNU-449 MOCK cells seeded on 24-well plates as 70 cells/well. The cells were cultured until single-cell colony formation. Cell culture media was refreshed in every three days and cells were incubated for one week. The day of analysis, cell culture media was aspirated and colonies were fixed with 1:1 cold Aceton : Methanol solution at -20^{o}C for 10 minutes. Colonies stained with 20% Giemsa solution for 20 minutes. After washing with distilled water, plate was incubated at room temperature for air dry. Plates were imaged under BIO-RAD Gel Doc™ XR+ Gel Documentation System and the images were analyzed via ImageJ - ColonyArea plug-in (29).

Phalloidin Staining

HCC cells were seeded on glass cover slips (22x22 cm) and incubated overnight for adhesion. Phalloidin (Abcam, abID#176756, USA)staining was performed as previously described (30). Imaging performed at IBG Optic Imaging Core Facility with fluorescent (Olympus - BX61) and Zeiss LSM 880-Confocal Laser Scanning Microscopy with Airyscan.

MTT Assay

SNU-449 HOTAIR OE and SNU-449 MOCK 1,000 cells per well were seeded on 96-well plate and incubated for 24, 48 and 72 hours. MTT analysis performed as described previously (31). Measured absorbance was analyzed by Microsoft Excel 2016 and plotted by Prism 8.

Analysis of TCGA and GEO microarray datasets

Normalized gene expression data from dataset GSE89377 was analyzed with GEO2R. Expression values plotted and statistically analyzed with Prism 8.

Zebrafish Xenograft Assay

Zebrafish xenograft assay was performed with SNU-449 MOCK and SNU-449 HOTAIR cell clones. The experiment was performed as described in a previous study (30). Briefly, 48hpf embryos were anesthetized and DiI labeled cells were injected to the yolk sack.100 cells per embryo were injected, successful injections to yolk with localized cells were selected 4 hours after injection. Xenografts were analyzed with Olympus SZX16 Fluorescent stereomicroscope. Three independent experiments were performed and each group consisted average number of 50 embryos with intact tumorospheres. All experiments were performed in compliance with local ethics regulations and EU Directive 2006 and approved by IBG Animal Ethics Committee with the protocol number of 03/2019.

Statistical Analysis

Statistical analysis performed using the GraphPad Prism 8 software. Statistical methods included Analysis of variance (ANOVA), Student's t-test and linear regression. Zebrafish xenograft data was statistically analyzed with chi-square with Yates correction as described in previous study (32). Results with $p<0.05$ were considered as statistically significant.

Results

Expression of HOTAIR is low in HCC cells with high c-Met expression and activation

To examine expression levels of HOTAIR and c-Met, we analyzed their mRNA expression in 10 HCC cell lines (FOCUS, SNU-449, SK-HEP-1, SNU-475, SNU-387, SNU-423, MAHLAVU, Hep-3B, HuH-7 and SNU-398). HOTAIR expression was only abundant in HuH-7 and SNU-398 cell lines which are also known to have low or no c-Met expression, respectively (Figure 1a-1b). To evaluate the potential relation between HOTAIR and c-Met protein expressions, we selected two cell lines with constitutive c-Met activation (SNU-449 and

SK-HEP-1) and two with low c-Met expression (HuH-7 and Hep-3B). RT-qPCR analysis of HOTAIR mRNA expression levels and western blot analysis of c-Met protein expression revealed that HOTAIR expression is low in HCC cell lines with high c-Met protein expression (Figure 1c). To understand the relationship between HOTAIR and c-Met expression in HCC, we analyzed HOTAIR and MET gene expression in a microarray dataset, GSE89377, which comprise gene expression analysis in patient tissues from normal liver, dysplasia, early and late HCC stages (33). Expression analysis of the dataset showed that HOTAIR expression decreases through HCC progression whereas MET gene expression increases (Figure 1d).

To evaluate the effect of ectopic HOTAIR expression on c-Met expressing HCC cells, we overexpressed HOTAIR in SNU-449 cell line which has constitutive c-Met activation. Overexpression of HOTAIR (HOTAIR OE) and its effect on c-Met expression were analyzed and confirmed with confocal microscopy imaging of fluorescent *in-situ* hybridization (FISH) of HOTAIR, immunofluorescent labeling of c-Met (Figure 1e), and also with RT-qPCR (Figure 1f). HOTAIR overexpression suppressed both mRNA and protein levels of c-Met, dramatically. To understand the possible interplay within two molecules in detail, we knocked down HOTAIR expression with siRNA transfection in HuH-7 cell line and then analyzed transcriptional and protein expression of c-Met. Analysis of three independent experiments showed that average of 45% knock-down of HOTAIR (Figure 1g) induced c-Met mRNA (Figure 1h) and protein expression (Figure 1i), significantly.

lncRNA HOTAIR overexpression suppresses c-Met downstream signaling and modulates its cellular localization via suppressing Caveolin-1 expression

To understand the effects of HOTAIR on c-Met signaling, we analyzed activation of c-Met and downstream signaling pathways Akt, MAPK and STAT3. Western blot analysis showed that HOTAIR OE suppressed both c-Met activity and protein expression (Figure 2a). HOTAIR OE caused a modest decrease in Akt activation (Figure 2b), and suppressed MAPK (Figure 2c) and STAT3 (Figure 2d) activations, dramatically. We confirmed these results by analyzing expression and activation of c-Met by immunofluorescent microscopy. Furthermore, immunofluorescent labeling revealed a differential organization and localization of c-Met in HOTAIR OE cells (Figure 2e). In our previous studies, we reported that Caveolin-1 (CAV1), a membrane protein enriched in lipid-rafts, contributes to c-Met activation and localization in HCC cells (27). To investigate the possible role of CAV1 in HOTAIR/c-Met interaction, we analyzed expression and activation of CAV1 and its activating kinase Src in HOTAIR OE cells. HOTAIR OE suppressed CAV1 mRNA level (Figure 2f), protein expression and activation (Figure 2g) as well as Src kinase expression and activation (Figure 2h). Moreover, membrane organization of Caveolin-1 was disrupted in HOTAIR OE cells which was compatible with disorganization of c-Met (Figure 2i).

Overexpression and/or activation of c-Met decreases HOTAIR expression in HCC cell lines

To understand the interplay between HOTAIR and c-Met further, we applied an opposite approach by overexpressing c-Met in SNU-398 HCC cell line which lacks c-Met protein expression and activation (Figure 1a). Overexpression and activation of c-Met were confirmed by western blot, immunofluorescent labeling and RT-qPCR analysis (Figure 3a, 3b). Analysis of HOTAIR expression in MET OE cells by FISH

and RT-qPCR showed that HOTAIR mRNA expression was significantly suppressed by c-Met overexpression (Figure 3c). To investigate HOTAIR/c-Met/Caveolin-1 relationship further, we analyzed Caveolin-1 expression in c-MET OE cell lines and found that Caveolin-1 expression was significantly upregulated, consistent with HOTAIR down-regulation (Figure 3d). Suppression of HOTAIR expression in MET OE cells was maintained not only by the elevation of protein expression, but also by the induction of both c-Met and Caveolin-1 activation (Figure 1d).

To understand the role of c-Met activation in HOTAIR expression, we analyzed the effects of HGF induced c-Met activation and/or its inhibition by a small molecule SU11274 in HuH-7 (Supplementary Figure 1b) and SNU-449 cell lines as well as SNU-449-MOCK and SNU-449-HOTAIR cells. HGF induction caused a significant decrease in HOTAIR transcript level in HCC cells, which was rescued by inhibition of c-Met activation by SU11274 (Supplementary Figure 1b, Figure 3e-h). We also examined the role of ligand-independent c-Met activation on HOTAIR transcription. In our previous studies, we showed that heparin treatment induces ligand independent c-Met activation in HCC cell lines (34). Similar to HGF, heparin induced c-Met activation resulted in a substantial decrease in HOTAIR transcription (Supplementary Figure 1c). Finally, we tested HOTAIR levels in sorafenib resistant HCC cell lines those generated in our previous studies (5). Consistent with elevated c-Met expression and activation, HOTAIR expression levels were significantly decreased in sorafenib resistant Mahlavu clones (Figure 3i). The maintenance of the interplay between HOTAIR and c-Met in different contexts shows that there is a reciprocal crosstalk between those molecules in HCC cell lines.

To understand the biological significance of this interaction, we investigated the phenotypic and biological results of HOTAIR overexpression in SNU-449 HCC cell line.

HOTAIR OE induced c-Met inhibition decreases adhesion, proliferation and colony formation of SNU-449 cells

HOTAIR OE cells showed reduced adhesion capacity to cell culture-treated (Figure 4a) and basal membrane extract coated cell culture surfaces (Figure 4b) in xCELLigence real time cell analysis system (RTCA). To understand the cause of decreased extracellular matrix (ECM) attachment capacity, we analyzed the expression of cell surface integrins that contribute to matrix attachment. ITGA6, ITGB1, ITGA4 and ITGB4 expressions were down-regulated in HOTAIR OE cells, significantly (Figure 4c).

Proliferation of the cells were evaluated with both xCELLigence RTCA system (Figure 4d) and MTT analysis (Figure 4e). HOTAIR OE cells showed significant reduction in proliferation rate in both techniques. Compatible with proliferation assays, 2D colony forming potential of HOTAIR OE cells were dramatically low. Colony counts normalized to number of cells plated for evaluation of colonization percentage. HOTAIR OE cells showed significantly lower colonization ability in comparison to MOCK cells (Figure 4f). Coverage area of colonies in well-plates, staining intensity of colonies and average colony sizes were also significantly lower in HOTAIR OE cells (Figure 4g-4j). These results reflect lower capacity of adhesion and proliferation.

HOTAIR OE induced c-Met inhibition decreases motility and invasion capacity of SNU-449 cells

Motility and invasion experiments were performed in parallel by both xCELLigence RTCA system and trans-well cell culture systems. Cell index of motile (Figure 5a) and invasive (Figure 5c) cells in HOTAIR OE clones were significantly lower in xCELLigence RTCA ($p \leq 0.001$). Consistent with real-time motility and invasion analysis; the number of motile and invasive cells migrated through trans-well cell culture inserts were reduced in HOTAIR OE cells (Figure 5b, 5d), significantly ($p \leq 0.05$).

Since trans-well systems especially tests individual cell movement ability, we further analyzed collective migration ability of clones in scratch (wound-healing) assay. Scratch assay enables cells to move collectively, without losing cell-cell attachments. Even though HOTAIR OE cells have reduced ability to migrate individually, they were still motile. Rather than migrating individually, HOTAIR OE cells migrated without losing cell-cell contacts, collectively (Figure 5e).

lncRNA HOTAIR inhibits c-Met induced cell scattering and promotes metastasis in zebrafish embryos

Decrease in attachment capacity to ECM led us to investigate spheroid formation capacity of HOTAIR OE cells. We analyzed spheroid formation ability of those cells with hanging-drop spheroid formation assay. SNU-449 cells have a complete mesenchymal phenotype, as a result of scattering effect of constitutive c-Met activation, and they are not inclined to form spheroids in hanging-drops. Due to their reduced ability to form cell-cell contacts maintained by constitutive c-Met activation; MOCK cells formed loose, scattered and wide clusters whereas HOTAIR OE cells formed more tight, stacked and small spheroids (Figure 6a). Significant ability to form intact spheroids led us to investigate their survival capacity under fluidic shear stress (FSS). To test their survival ability, cells sheared for 1 hour under FSS of 0.5 dyn/cm^2, mimicking the sinusoidal shear stress in liver (35). HOTAIR OE improved survival ability under sinusoidal FSS. Alive cell numbers after one hour of FSS was significantly higher ($p \leq 0.05$) in HOTAIR OE clones (Figure 6b).

Finally, embryonic zebrafish xenograft model was used to test in vivo metastatic capacity of HOTAIR OE, further. Average number of 100 HOTAIR OE and MOCK cells were injected to the yolk sac of 48h zebrafish embryos and embryos which bear an intact tumorosphere after 4 hours of injection were incubated for 4 days to analyze metastatic capacity (Figure 6c). Three independent experiments were performed and in every experiment each group consisted average number of 50 embryos with intact tumorospheres. Even wild-type SNU-449 cells known to be highly metastatic in embryonic zebrafish model, HOTAIR OE dramatically increased their metastatic capacity when compared to MOCK cells (Figure 6d).

lncRNA HOTAIR maintains hybrid E/M phenotype to promote metastasis

Our experiments with HOTAIR OE cells show morphological and biological properties that are consistent with the hybrid E/M phenotype which can be defined as a fluidic state between epithelial and mesenchymal phenotypes (Figure 7a). To test this hypothesis, we examined previously defined EMT markers in HOTAIR OE SNU-449 cells (36-38). First, we found that in contrary to the mesenchymal and elongated phenotype, HOTAIR OE cells were round-shaped with thinner F-actin stress fibrils indicated with

phalloidin staining (Figure 7b). Then, we performed a detailed investigation of molecular biomarkers of hybrid E/M phenotype. In HOTAIR OE cells, beta-catenin was enriched in the plasma membrane (Figure 7c), expression of epithelial biomarker E-cadherin was upregulated (Figure 7d) whereas mesenchymal biomarker Vimentin expression was significantly down-regulated and showed polarity (Figure 7e). Consistent with epithelial phenotype, N-Cadherin expression was down-regulated and mostly located in the plasma membrane of HOTAIR OE cells (Figure 7f). Immunofluorescent analysis of cytoskeletal organization of F-actin and Vimentin in MET OE clones showed that ectopic MET expression and its suppressive effect on HOTAIR expression was also resulted in thickening of F-actin stress fibrils, and increase in Vimentin expression and polarity (Supplementary Figure 1d).

Finally, we analyzed TCGA datasets of various cancers to have a foresight about the possible relationship of two molecules (3). HOTAIR and MET gene transcripts in TCGA datasets were analyzed by UALCAN (39). HOTAIR and c-Met were differentially expressed between normal and primary tumor tissues and they were reversely correlated with each other in breast invasive carcinoma (BRCA), cervical squamous cell carcinoma (CESC), sarcoma (SARC) and skin cutaneous melanoma (SKCM) cancer types (Figure 8a-8e). Although lncRNA HOTAIR, one of the most studied long non-coding RNAs, is reported to be elevated in patients with metastasis and poor prognosis in many cancer types, analysis of HOTAIR in TCGA datasets revealed that HOTAIR has a context-dependent expression pattern which is not always upregulated through the progression of the disease (Supplementary Figure 2).

Discussion

Our results suggest c-Met and HOTAIR axis as a modulator of epithelial/mesenchymal hybrid state in hepatocellular carcinoma cells. Mechanistically, we demonstrated that the interplay between c-Met receptor tyrosine kinase and HOTAIR is critical for maintenance of hybrid E/M state in HCC cells to cope with rate-limiting steps of tumor metastasis, such as survival in adhesion independent microenvironment, escaping from anoikis and resisting to fluidic shear stress (FSS) in HCC.

HCC cell lines with high c-Met expression and activation are defined to have mesenchymal phenotype in previous definitive studies (40, 41). In our study, we report that HCC cells can be divided into two clusters which show differential expression tendency for HOTAIR and c-MET genes. Expression of these two molecules among 10 HCC cell lines demonstrated that most HCC cell lines show a reverse tendency in levels of c-Met and HOTAIR expression. To further confirm the possible reverse interaction between HOTAIR and c-Met, we overexpressed HOTAIR in SNU-449 cell line which has ligand-independent constitutive c-Met activation, and silenced HOTAIR in HuH-7 cell line which expresses HOTAIR, abundantly. Our results show that constitutive c-Met expression is suppressed by HOTAIR over-expression and HOTAIR silencing induced c-Met expression in HCC cells.

Analysis of microarray dataset comprised of tissues from normal liver, dysplastic liver, early and late HCC of patients (GSE89377) showed that HOTAIR was downregulated through hepatocarcinogenesis whereas c-Met expression was upregulated. This analysis supports our data showing HOTAIR downregulation is a

requirement for c-Met activation and c-Met triggered complete mesenchymal phenotype in HCC cell lines. Contrary to the reports of melanoma, retinoblastoma and colon cancer studies (42–44) and expectations on the parallel expression tendencies of c-Met and HOTAIR in HCC cell lines; comparative analysis of HCC cell lines and cancer datasets shows the opposite, clearly. Indicated studies suggested HOTAIR as a competing long non-coding RNA decoying microRNAs targeting c-Met in different cancer contexts, and those microRNAs are reported to have different molecular targets in HCC rather than c-Met (45, 46).

In addition to suppression of c-Met, HOTAIR weakens downstream Akt1, MAPK and STAT3 signaling pathways not only by decreasing c-Met expression but also by modulating its membrane organization. In our previous studies, we showed that Caveolin-1 enhances c-Met signaling by co-localizing in plasma membrane (27). Src kinase, a well-identified downstream effector of c-Met, phosphorylates Caveolin-1 from Tyr-14 residue to induce lipid-raft enrichment of c-Met with Caveolin-1 and formation of caveola structures (27, 47). HOTAIR over-expression reduced Caveolin-1 expression and activation via suppressing activation of c-Met and its downstream effector Src kinase. In parallel to c-Met, Caveolin-1 organization in plasma membrane was also disrupted in HOTAIR OE cells. Tsai et. al defined function of HOTAIR in epigenetic regulation of its target genes and they reported Caveolin-1 as one of the most differentially expressed genes in response to HOTAIR knock-down in foreskin fibroblasts (12). We confirmed the interaction axis of c-Met, HOTAIR and Caveolin-1 is conserved in c-Met over-expression model of SNU-398 cell line its wild type is lack of c-Met expression but expresses HOTAIR, abundantly. In addition to the lack of c-Met expression, SNU-398 cells also do not express Caveolin-1 (26). As a consequence of c-Met overexpression and HOTAIR suppression, Caveolin-1 expression was induced in those cells. In addition to the over-expression studies of c-Met and HOTAIR, we showed that c-Met and HOTAIR reverse interaction is conserved in both ligand-dependent and independent c-Met activation contexts. These results support the defined interplay between two molecules.

To understand the biological significance of HOTAIR/c-Met interaction, we analyzed the results of HOTAIR overexpression on c-Met related biological responses which are clearly defined in the literature as contributing to aggressive phenotype of HCC cells (48). HOTAIR over-expressing cells showed delayed adhesion to surfaces and suppressed expression of adhesion-related integrins (49). In addition to decreased attachment to surface, proliferation and colony formation ability of HOTAIR OE cells were decreased. Suppression of individual motility and invasion of HOTAIR OE cells were consistent with suppressed scattering effect of c-Met signaling. HOTAIR OE cells were migrating collectively rather than individually which is compatible with previous studies explaining migration behavior of cells with hybrid E/M phenotype (15). Increased expression of cell adhesion molecules such as CDH-1 and JAM-2 (Supplementary Fig. 1a) were consistent with the evidence of collective migration that requires preservation of cell-to-cell interactions (50, 51).

Surprisingly, HOTAIR over-expressing cells showed increased survival ability in adhesion independent culture and under FSS. Escaping from anoikis and overcoming damage incurred by shear forces are important necessities of survival in circulation to achieve metastasis (52). Response to fluidic shear-stress or adhesion-independent conditions are context-dependent processes those depend on the

molecular pool of the cell; HOTAIR over-expressing cells resisted those unfavorable conditions via formation of spheres (35). Aggregation into spheroids to overcome the stress of unfavorable microenvironment, enhancing cell-cell adhesion and surviving under damage of shear forces are well-defined requirements of metastasis (35, 52). As expected, by attainment of those abilities, HOTAIR over-expression increased metastatic ability of SNU-449 cells which was defined to be highly metastatic in our previous studies in zebrafish xenograft model (30). Our study is the first in the literature defining the molecular basis of HOTAIR overexpression mediated increase in the metastatic ability of HCC cells.

Since the definition of EMT has been changed and broadened, transitional states between epithelial and mesenchymal phenotypes are called “partial EMT”. Existence of intermediate hybrid phenotypes have been defined in different molecular and biological processes such as fibrosis, development, wound healing and cancer (15). In our study, we found that HOTAIR acts as a fine tuner of maintenance of hybrid E/M phenotype by modulating c-Met signaling. Compatibly with the literature, we analyzed defined morphological and molecular markers of epithelial and mesenchymal phenotypes in HOTAIR over-expressing cells (15, 16, 37, 38). HOTAIR OE cells were round-shaped and had thinner F-actin stress fibrils. beta-Catenin was enriched in membrane compatible with increased E-cadherin expression and hybrid E/M phenotype characteristics (18). In comparison with MOCK cells, mesenchymal biomarkers Vimentin and N-cadherin expression was suppressed in HOTAIR OE cells (Fig. 7). Changes in cytoskeletal components and dis-/re-assembling of cell-cell contacts regulates gene expression, motility and cell-cycle. Cells placed in spectrum between epithelial and mesenchymal phenotypes are reported to arrest cell cycle and decrease their proliferative activity (15, 17). Consistent with the literature, proliferation rate of HOTAIR OE cells were decreased (Fig. 4) and cell cycle was arrested (Supplementary Fig. 1e).

Decrease in biological responses such as individual cell motility and invasion are consistent with suppressed scattering effect of c-Met signaling activity. Even individual cell motility was decreased, HOTAIR OE clones have ability to enclose the scratch via collective migration as fast as MOCK clones in wound-healing assay (Fig. 5). Collective migration is not only important for maintenance of invading front of tumors but also it is an emerging mechanism for seeding of secondary tumors (53). Taken together, our data shows that decrease in HOTAIR expression and its effects on c-Met and Caveolin-1 activation is crucial through the completion of mesenchymal phenotype.

Concordant with our data, we report that c-Met and HOTAIR expression profiles show inverse tendencies in breast invasive carcinoma (BRCA), cervical squamous cell carcinoma (CESC), sarcoma (SARC), skin cutaneous melanoma (SKCM) and sarcoma (SARC) (Supplementary Fig. 2).

Our study clearly defines the fine tuning of c-Met signaling by HOTAIR to maintain hybrid E/M phenotype which ensures flexibility of commitment and enhances metastatic ability under unfavorable conditions through rate-limiting steps of metastasis. Further studies are needed to address the molecular cascade between HOTAIR, c-Met and Caveolin-1 in detail.

Conclusions

In conclusion, HOTAIR over-expression suppresses c-Met expression, activation and also disrupts its organization on plasma membrane by modulating Caveolin-1 expression and activation. HOTAIR over-expression provides an advantage to HCC cells via maintaining hybrid E/M phenotype thereby enhancing survival in adhesion-independent and shear-stressed conditions. HOTAIR overexpression decreases adhesion dependency and proliferation while increasing spheroid formation and improving collective migration abilities and overall improving metastatic potential of HCC cells. Further studies are needed to brighten detailed regulatory signaling cascades and mapping potential targets for therapeutic applications.

Abbreviations

CTCs: Circulating Tumor Cells

EMT: Epithelial to mesenchymal transition

FSS: Fluidic Shear Stress

GBD: Global Burden of Disease

HCC: Hepatocellular Carcinoma

HOTAIR: HOX Transcript Antisense Intergenic RNA

lncRNA: long non-coding RNA

MET: Mesenchymal to epithelial transition

OE: Over-expression

RT: Room temperature

RT-qPCR: Reverse transcriptase-quantitative polymerase chain reaction

RTCA: Real time cell analysis system

TCGA: The Cancer Genome Atlas

Declarations

Ethics approval and consent to participate

In vitro experiments of this study were approved by Non-Interventional Research Ethics Board of Dokuz Eylül University with the protocol number of 1597-GOA. Animal experiments of this study was approved by IBG Animal Ethics Committee with the protocol number of 03/2019.

Consent for Publication

Not applicable.

Availability of Data and Material

Eun et al., 2016, performed expression profiling array to identify novel drivers of hepatocellular carcinoma and reveal clinical relevance as early diagnostic and prognostic biomarkers (data accessible at NCBI GEO database (Eun et al., 2016), accession GSE89377). https://www.ncbi.nlm.nih.gov/geo/query/acc.cgi?acc=GSE89377

The results reported here are in whole or part based upon data generated by the TCGA Research Network: https://www.cancer.gov/tcga.

Competing Interests

The authors declare that they have no competing interests.

Funding

This research was funded by “Department of Scientific Research Projects of Dokuz Eylul University (BAP), grant number 2016.KB.SAG.005” and “Scientific and Technological Research Council of Turkey (TUBITAK), grant number 114S359“. HT was awarded with a Short-Term Fellowship from the European Molecular Biology Organization (EMBO) between 01.06.17-01.07.17.

Author Contributions

HT, EB, DC and GB performed the experiments. HT performed data analysis and curation. GCA supervised and trained HT for Zebrafish xenograft model establishment and performance. HT and NA conceived the experiments and study plan. Data was mainly interpreted by HT and NA. EB, DC and GB contributed experiment discussions. HT prepared the original draft and NA performed review edit of the manuscript. NA performed supervision, project administration and funding acquisitions.

All authors read and approved the final manuscript.

Acknowledgments

We thank Prof. Dr. Mehmet Öztürk for providing HCC cells and Izmir Biomedicine and Genome Center for establishment of required technical and instrumental infrastructure for this study. We thank IBG Vivarium Zebrafish facility for housing and providing the animals, Melek Ucuncu and Didem Cimtay from IBG Optical Imaging Core Facility for their supports for imaging processes of samples.

Materials & Correspondence:

Requests should be addressed to Nese Atabey (nese.atabey@ibg.edu.tr) or Hande Topel (handetb@bmb.sdu.dk).

References

1. Global Burden of Disease Cancer C, Fitzmaurice C, Abate D, Abbasi N, Abbastabar H, Abd-Allah F, et al. Global, Regional, and National Cancer Incidence, Mortality, Years of Life Lost, Years Lived With Disability, and Disability-Adjusted Life-Years for 29 Cancer Groups, 1990 to 2017: A Systematic Analysis for the Global Burden of Disease Study. JAMA Oncol. 2019.
2. Yang JD, Hainaut P, Gores GJ, Amadou A, Plymoth A, Roberts LR. A global view of hepatocellular carcinoma: trends, risk, prevention and management. Nat Rev Gastroenterol Hepatol. 2019;16(10):589-604.
3. Cancer Genome Atlas Research Network. Electronic address wbe, Cancer Genome Atlas Research N. Comprehensive and Integrative Genomic Characterization of Hepatocellular Carcinoma. Cell. 2017;169(7):1327-41 e23.
4. Bouattour M, Raymond E, Qin S, Cheng AL, Stammberger U, Locatelli G, et al. Recent developments of c-Met as a therapeutic target in hepatocellular carcinoma. Hepatology. 2018;67(3):1132-49.
5. Firtina Karagonlar Z, Koc D, Iscan E, Erdal E, Atabey N. Elevated hepatocyte growth factor expression as an autocrine c-Met activation mechanism in acquired resistance to sorafenib in hepatocellular carcinoma cells. Cancer Sci. 2016;107(4):407-16.
6. Rinn JL, Kertesz M, Wang JK, Squazzo SL, Xu X, Brugmann SA, et al. Functional demarcation of active and silent chromatin domains in human HOX loci by noncoding RNAs. Cell. 2007;129(7):1311-23.
7. Gupta RA, Shah N, Wang KC, Kim J, Horlings HM, Wong DJ, et al. Long non-coding RNA HOTAIR reprograms chromatin state to promote cancer metastasis. Nature. 2010;464(7291):1071-6.
8. Deng J, Yang M, Jiang R, An N, Wang X, Liu B. Long Non-Coding RNA HOTAIR Regulates the Proliferation, Self-Renewal Capacity, Tumor Formation and Migration of the Cancer Stem-Like Cell (CSC) Subpopulation Enriched from Breast Cancer Cells. PLoS One. 2017;12(1):e0170860.
9. Liu XH, Liu ZL, Sun M, Liu J, Wang ZX, De W. The long non-coding RNA HOTAIR indicates a poor prognosis and promotes metastasis in non-small cell lung cancer. BMC Cancer. 2013;13:464.
10. Tan SK, Pastori C, Penas C, Komotar RJ, Ivan ME, Wahlestedt C, et al. Serum long noncoding RNA HOTAIR as a novel diagnostic and prognostic biomarker in glioblastoma multiforme. Mol Cancer. 2018;17(1):74.
11. Wang W, He X, Zheng Z, Ma X, Hu X, Wu D, et al. Serum HOTAIR as a novel diagnostic biomarker for esophageal squamous cell carcinoma. Mol Cancer. 2017;16(1):75.
12. Tsai MC, Manor O, Wan Y, Mosammaparast N, Wang JK, Lan F, et al. Long noncoding RNA as modular scaffold of histone modification complexes. Science. 2010;329(5992):689-93.

13. Tang X, Feng D, Li M, Zhou J, Li X, Zhao D, et al. Transcriptomic Analysis of mRNA-lncRNA-miRNA Interactions in Hepatocellular Carcinoma. Sci Rep. 2019;9(1):16096.
14. Somarowthu S, Legiewicz M, Chillon I, Marcia M, Liu F, Pyle AM. HOTAIR forms an intricate and modular secondary structure. Mol Cell. 2015;58(2):353-61.
15. Nieto MA, Huang RY, Jackson RA, Thiery JP. Emt: 2016. Cell. 2016;166(1):21-45.
16. Denisov EV, Perelmuter VM. A fixed partial epithelial-mesenchymal transition (EMT) triggers carcinogenesis, whereas asymmetrical division of hybrid EMT cells drives cancer progression. Hepatology. 2018;68(3):807-10.
17. Lovisa S, LeBleu VS, Tampe B, Sugimoto H, Vadnagara K, Carstens JL, et al. Epithelial-to-mesenchymal transition induces cell cycle arrest and parenchymal damage in renal fibrosis. Nat Med. 2015;21(9):998-1009.
18. Basu S, Cheriyamundath S, Ben-Ze'ev A. Cell-cell adhesion: linking Wnt/beta-catenin signaling with partial EMT and stemness traits in tumorigenesis. F1000Res. 2018;7.
19. Lecharpentier A, Vielh P, Perez-Moreno P, Planchard D, Soria JC, Farace F. Detection of circulating tumour cells with a hybrid (epithelial/mesenchymal) phenotype in patients with metastatic non-small cell lung cancer. Br J Cancer. 2011;105(9):1338-41.
20. Armstrong AJ, Marengo MS, Oltean S, Kemeny G, Bitting RL, Turnbull JD, et al. Circulating tumor cells from patients with advanced prostate and breast cancer display both epithelial and mesenchymal markers. Mol Cancer Res. 2011;9(8):997-1007.
21. Revenu C, Gilmour D. EMT 2.0: shaping epithelia through collective migration. Curr Opin Genet Dev. 2009;19(4):338-42.
22. Grosse-Wilde A, Fouquier d'Herouel A, McIntosh E, Ertaylan G, Skupin A, Kuestner RE, et al. Stemness of the hybrid Epithelial/Mesenchymal State in Breast Cancer and Its Association with Poor Survival. PLoS One. 2015;10(5):e0126522.
23. Almale L, Garcia-Alvaro M, Martinez-Palacian A, Garcia-Bravo M, Lazcanoiturburu N, Addante A, et al. c-Met Signaling Is Essential for Mouse Adult Liver Progenitor Cells Expansion After Transforming Growth Factor-beta-Induced Epithelial-Mesenchymal Transition and Regulates Cell Phenotypic Switch. Stem Cells. 2019;37(8):1108-18.
24. Yang Z, Zhou L, Wu LM, Lai MC, Xie HY, Zhang F, et al. Overexpression of long non-coding RNA HOTAIR predicts tumor recurrence in hepatocellular carcinoma patients following liver transplantation. Ann Surg Oncol. 2011;18(5):1243-50.
25. Ishibashi M, Kogo R, Shibata K, Sawada G, Takahashi Y, Kurashige J, et al. Clinical significance of the expression of long non-coding RNA HOTAIR in primary hepatocellular carcinoma. Oncol Rep. 2013;29(3):946-50.
26. Cokakli M, Erdal E, Nart D, Yilmaz F, Sagol O, Kilic M, et al. Differential expression of Caveolin-1 in hepatocellular carcinoma: correlation with differentiation state, motility and invasion. BMC Cancer. 2009;9:65.

27. Korhan P, Erdal E, Kandemis E, Cokakli M, Nart D, Yilmaz F, et al. Reciprocal activating crosstalk between c-Met and caveolin 1 promotes invasive phenotype in hepatocellular carcinoma. PLoS One. 2014;9(8):e105278.
28. Gunes A, Iscan E, Topel H, Avci ST, Gumustekin M, Erdal E, et al. Heparin treatment increases thioredoxin interacting protein expression in hepatocellular carcinoma cells. Int J Biochem Cell Biol. 2015;65:169-81.
29. Guzman C, Bagga M, Kaur A, Westermarck J, Abankwa D. ColonyArea: an ImageJ plugin to automatically quantify colony formation in clonogenic assays. PLoS One. 2014;9(3):e92444.
30. Gunes A, Bagirsakci E, Iscan E, Cakan-Akdogan G, Aykutlu U, Senturk S, et al. Thioredoxin interacting protein promotes invasion in hepatocellular carcinoma. Oncotarget. 2018;9(96):36849-66.
31. Bagirsakci E, Sahin E, Atabey N, Erdal E, Guerra V, Carr BI. Role of Albumin in Growth Inhibition in Hepatocellular Carcinoma. Oncology. 2017;93(2):136-42.
32. Avci ME, Keskus AG, Targen S, Isilak ME, Ozturk M, Atalay RC, et al. Development of a novel zebrafish xenograft model in ache mutants using liver cancer cell lines. Sci Rep. 2018;8(1):1570.
33. Eun J, Nam, S. Identifying novel drivers of human hepatocellular carcinoma and revealing clinical relevance as early diagnostic and prognostic biomarker. In: Korea TCUo, editor. South KoreaDec 31, 2017.
34. Iscan E, Gunes A, Korhan P, Yilmaz Y, Erdal E, Atabey N. The regulatory role of heparin on c-Met signaling in hepatocellular carcinoma cells. J Cell Commun Signal. 2017;11(2):155-66.
35. Huang Q, Hu X, He W, Zhao Y, Hao S, Wu Q, et al. Fluid shear stress and tumor metastasis. Am J Cancer Res. 2018;8(5):763-77.
36. Jolly MK, Somarelli JA, Sheth M, Biddle A, Tripathi SC, Armstrong AJ, et al. Hybrid epithelial/mesenchymal phenotypes promote metastasis and therapy resistance across carcinomas. Pharmacol Ther. 2019;194:161-84.
37. Kroger C, Afeyan A, Mraz J, Eaton EN, Reinhardt F, Khodor YL, et al. Acquisition of a hybrid E/M state is essential for tumorigenicity of basal breast cancer cells. Proc Natl Acad Sci U S A. 2019;116(15):7353-62.
38. Jolly MK, Boareto M, Huang B, Jia D, Lu M, Ben-Jacob E, et al. Implications of the Hybrid Epithelial/Mesenchymal Phenotype in Metastasis. Front Oncol. 2015;5:155.
39. Chandrashekar DS, Bashel B, Balasubramanya SAH, Creighton CJ, Ponce-Rodriguez I, Chakravarthi B, et al. UALCAN: A Portal for Facilitating Tumor Subgroup Gene Expression and Survival Analyses. Neoplasia. 2017;19(8):649-58.
40. Hirschfield H, Bian CB, Higashi T, Nakagawa S, Zeleke TZ, Nair VD, et al. In vitro modeling of hepatocellular carcinoma molecular subtypes for anti-cancer drug assessment. Exp Mol Med. 2018;50(1):e419.
41. Yuzugullu H, Benhaj K, Ozturk N, Senturk S, Celik E, Toylu A, et al. Canonical Wnt signaling is antagonized by noncanonical Wnt5a in hepatocellular carcinoma cells. Mol Cancer. 2009;8:90.

42. Luan W, Li R, Liu L, Ni X, Shi Y, Xia Y, et al. Long non-coding RNA HOTAIR acts as a competing endogenous RNA to promote malignant melanoma progression by sponging miR-152-3p. Oncotarget. 2017;8(49):85401-14.
43. Yang G, Fu Y, Lu X, Wang M, Dong H, Li Q. LncRNA HOTAIR/miR-613/c-met axis modulated epithelial-mesenchymal transition of retinoblastoma cells. J Cell Mol Med. 2018;22(10):5083-96.
44. Liu B, Liu Q, Pan S, Huang Y, Qi Y, Li S, et al. The HOTAIR/miR-214/ST6GAL1 crosstalk modulates colorectal cancer procession through mediating sialylated c-Met via JAK2/STAT3 cascade. J Exp Clin Cancer Res. 2019;38(1):455.
45. Jiang X, Wu J, Zhang Y, Wang S, Yu X, Li R, et al. MiR-613 functions as tumor suppressor in hepatocellular carcinoma by targeting YWHAZ. Gene. 2018;659:168-74.
46. Wang W, Zhang H, Wang L, Zhang S, Tang M. miR-613 inhibits the growth and invasiveness of human hepatocellular carcinoma via targeting DCLK1. Biochem Biophys Res Commun. 2016;473(4):987-92.
47. Gottlieb-Abraham E, Shvartsman DE, Donaldson JC, Ehrlich M, Gutman O, Martin GS, et al. Src-mediated caveolin-1 phosphorylation affects the targeting of active Src to specific membrane sites. Mol Biol Cell. 2013;24(24):3881-95.
48. Garcia-Vilas JA, Medina MA. Updates on the hepatocyte growth factor/c-Met axis in hepatocellular carcinoma and its therapeutic implications. World J Gastroenterol. 2018;24(33):3695-708.
49. Sokeland G, Schumacher U. The functional role of integrins during intra- and extravasation within the metastatic cascade. Mol Cancer. 2019;18(1):12.
50. Aurrand-Lions M, Johnson-Leger C, Wong C, Du Pasquier L, Imhof BA. Heterogeneity of endothelial junctions is reflected by differential expression and specific subcellular localization of the three JAM family members. Blood. 2001;98(13):3699-707.
51. Zhao H, Yu H, Martin TA, Zhang Y, Chen G, Jiang WG. Effect of junctional adhesion molecule-2 expression on cell growth, invasion and migration in human colorectal cancer. Int J Oncol. 2016;48(3):929-36.
52. Valastyan S, Weinberg RA. Tumor metastasis: molecular insights and evolving paradigms. Cell. 2011;147(2):275-92.
53. Campbell K, Casanova J. A common framework for EMT and collective cell migration. Development. 2016;143(23):4291-300.

Supplementary Materials:

Supplementary Figure 1: Includes supplementary data indicated in the text.

Supplementary Figure 2: The results shown in supplementary figure 2 are a part based upon data generated by the TCGA Research Network: https://www.cancer.gov/tcga. Data extracted from TCGA via UALCAN.

Supplementary document 1: Includes primer sequences used in gene expression analysis and catalog numbers of antibodies used in immunoblotting and/or immunofluorescent labeling experiments.

Figures

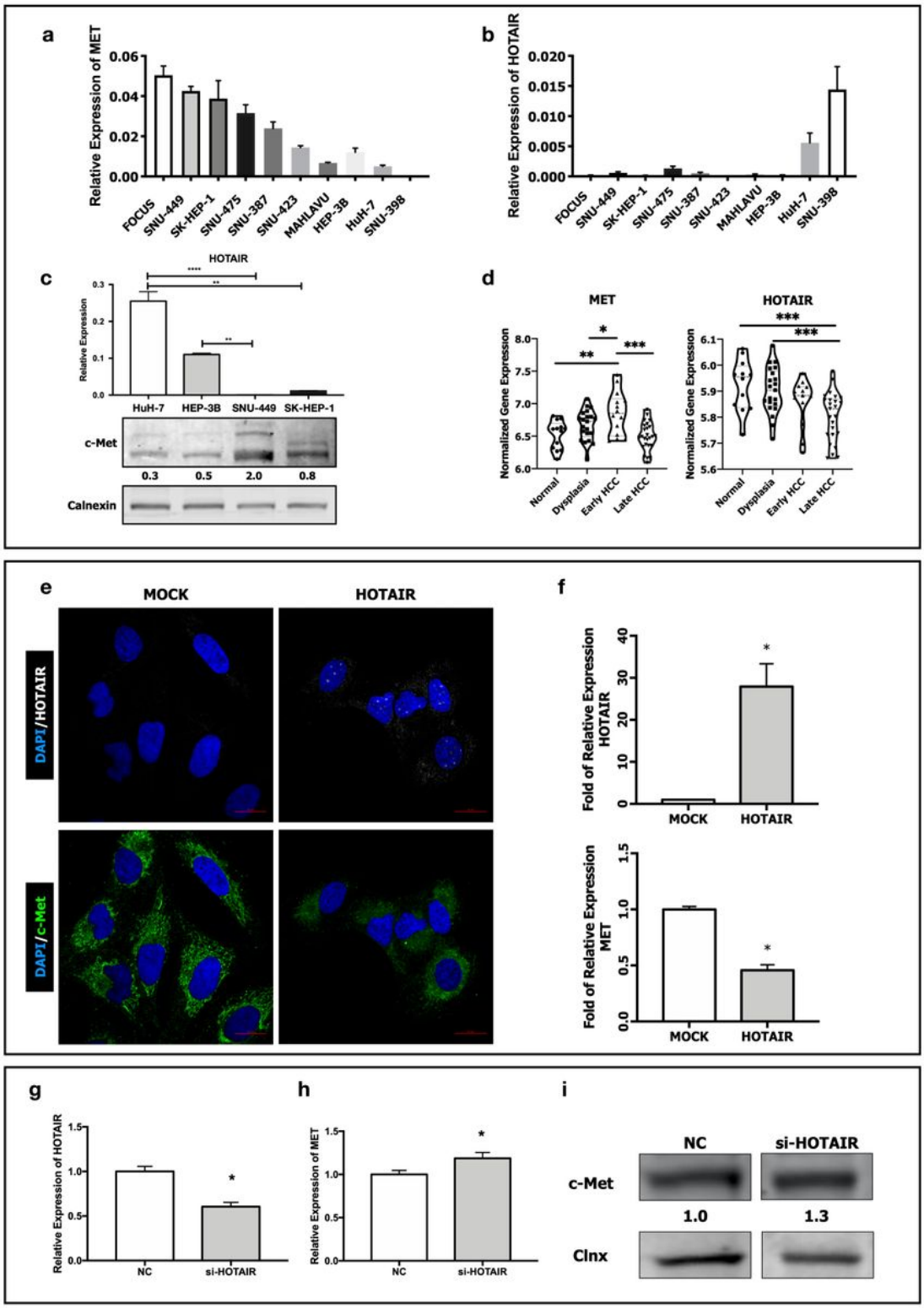

Figure 1

Expression of HOTAIR and c-Met in HCC cell lines and HCC progression RT-qPCR analysis of (a) MET and (b) HOTAIR expressions in HCC cell lines FOCUS, SNU-449, SK-HEP-1, SNU-475, SNU-387, SNU-423, MAHLAVU, Hep-3B, HuH-7 and SNU-398. (c) RT-qPCR analysis of HOTAIR expression and immunoblotting of c-Met protein in HuH-7, Hep-3B, SNU-449 and SK-HEP-1 cells. (d) Normalized expression levels of MET and HOTAIR in normal, dysplasia, early and late HCC tissues in microarray dataset GSE89377. (e) Confocal microscopy image of fluorescent-in-situ hybridized HOTAIR mRNA and immunofluorescent labeled c-Met protein expression in control (MOCK) and HOTAIR over-expressing (HOTAIR OE) SNU-449 cells. RT-qPCR analysis of (f) MET and HOTAIR mRNA expression in MOCK and HOTAIR OE clones. RT-qPCR analysis of (g) HOTAIR and (h) c-Met mRNA expression in control si-RNA (NC) and si-HOTAIR transfected HuH-7 cells. Western blot analysis of (i) c-Met protein expression in control (NC) and si-HOTAIR transfected HuH-7 cells. Densitometric analysis of band intensities in immunoblots were analyzed with ImageJ and normalized with internal control protein band intensities. All graphs of experiments are presented as the mean ± SEM of at least 3 independent experiments. * $p \leq 0.05$, ** $p \leq 0.01$, *** $p \leq 0.001$, **** $p \leq 0.0001$.

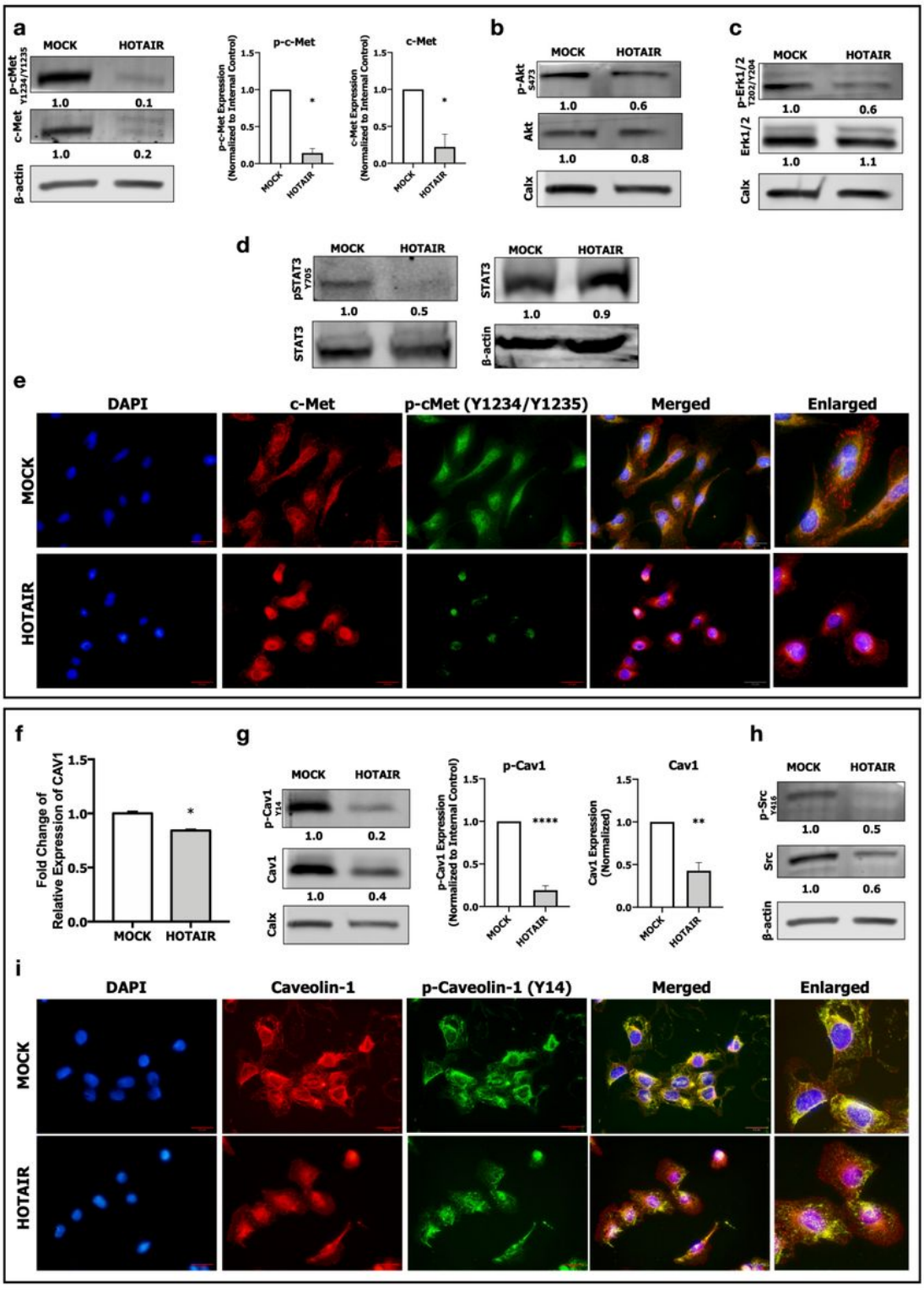

Figure 2

Effect of HOTAIR overexpression in c-Met downstream signaling Analysis of c-Met and downstream signaling in MOCK and HOTAIR OE cells. Immunoblot analysis of (a) c-Met protein expression, c-Met activation phosphorylation (Tyr-1234/Tyr-1235); (b) Akt1 protein expression, Akt1 activation phosphorylation (Ser-473); (c) Erk1/2 protein expression, Erk1/2 activation phosphorylation (Thr-202/Tyr-204); (d) STAT3 protein expression and activation phosphorylation (Tyr-705). Immunofluorescence

imaging of (e) total c-Met protein (red) and its activation (green). RT- qPCR analysis of (f) CAV1 mRNA expression and immunoblotting of (g) Caveolin-1 protein and its activation phosphorylation (Tyr-14). Immunoblotting of (h) Src kinase expression and its activation phosphorylation (Tyr-416). Immunofluorescence imaging of (i) total Caveolin-1 protein (red) and its activation (green). DAPI (blue) was used as nuclear marker in immunofluorescent images. Densitometric analysis of band intensities in immunoblots were analyzed with ImageJ and normalized with internal control protein band intensities. All graphs of experiments are presented as the mean ± SEM of at least 3 independent experiments. * $p \leq 0.05$, ** $p \leq 0.01$, *** $p \leq 0.001$, **** $p \leq 0.0001$.

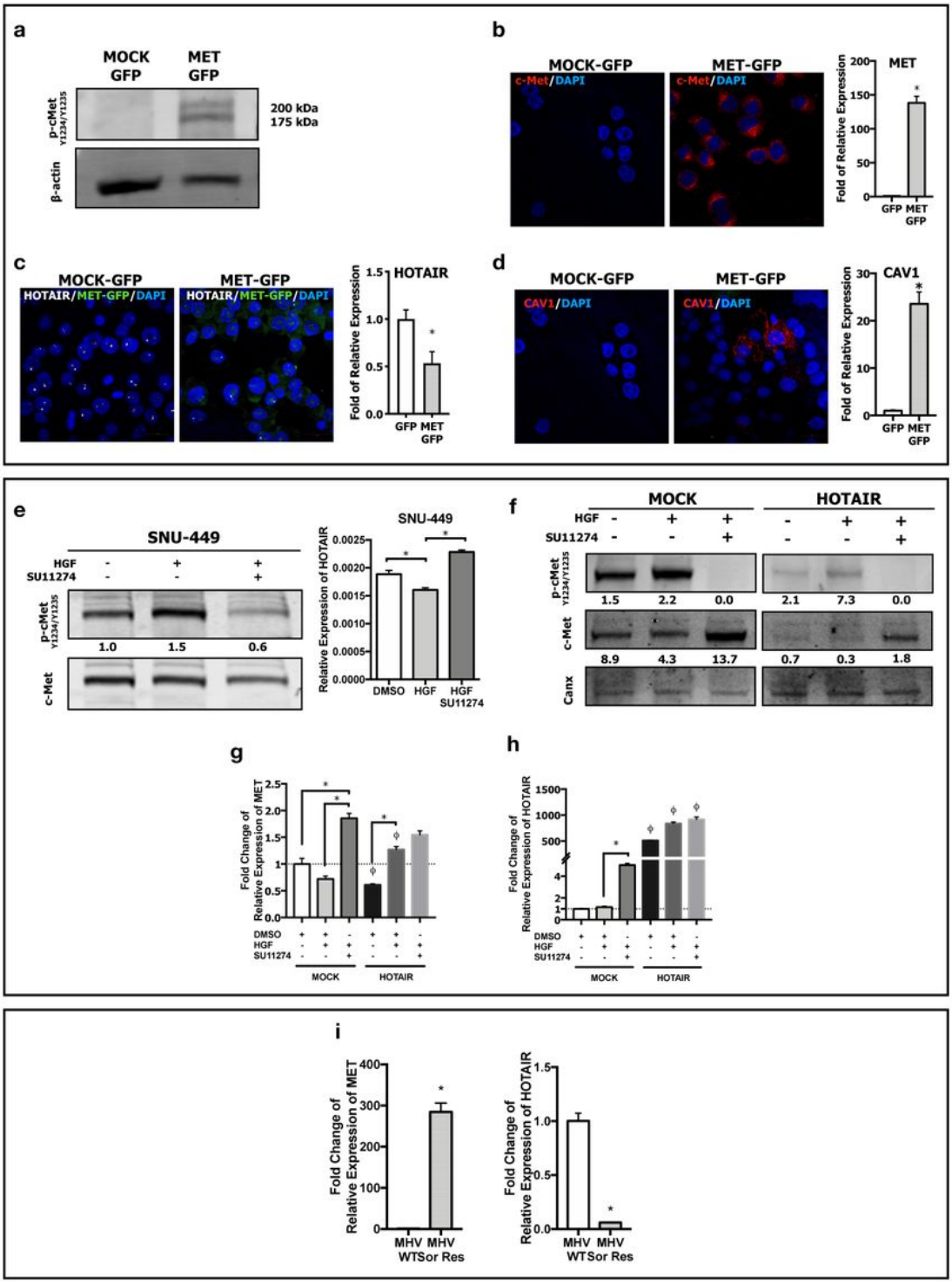

Figure 3

Analysis of HOTAIR-c-Met interaction in MET overexpressed, activated and inhibited conditions Immunoblotting of (a) c-Met activation, (b) confocal microscopy imaging of c-Met protein and RT-qPCR analysis of c-Met mRNA expression in MET OE SNU-398 clones. (c) Confocal imaging of FISH labeling (white dots) and RT-qPCR analysis of HOTAIR mRNA expression in MET OE clones. (d) Confocal imaging of Caveolin-1 protein and qPCR analysis of CAV1 mRNA expression in MET OE cells. (e) Immunoblot of c-

Met activation and qPCR analysis of HOTAIR expression in ligand-dependent activation (HGF 10 ng/ml) and kinase activity inhibition (SU11274, 2500 nM, small molecule c-Met inhibitor) of c-Met in wild-type SNU-449 cells. (f) Immunoblotting of c-Met activation and expression; RT-qPCR analysis of (g) MET and (h) HOTAIR expression in ligand-dependent activation (HGF) and kinase activity inhibition (SU11274) in MOCK and HOTAIR OE clones. Analysis of (i) HOTAIR and MET expression in response to ligand independent c-Met activation mechanism, sorafenib resistance. Densitometric analysis of band intensities in immunoblots were analyzed with ImageJ and normalized with internal control protein band intensities. All graphs of experiments are presented as the mean ± SEM of at least 3 independent experiments. * p≤ 0.05. φ: statistically significant in comparison with the same condition of MOCK clones.

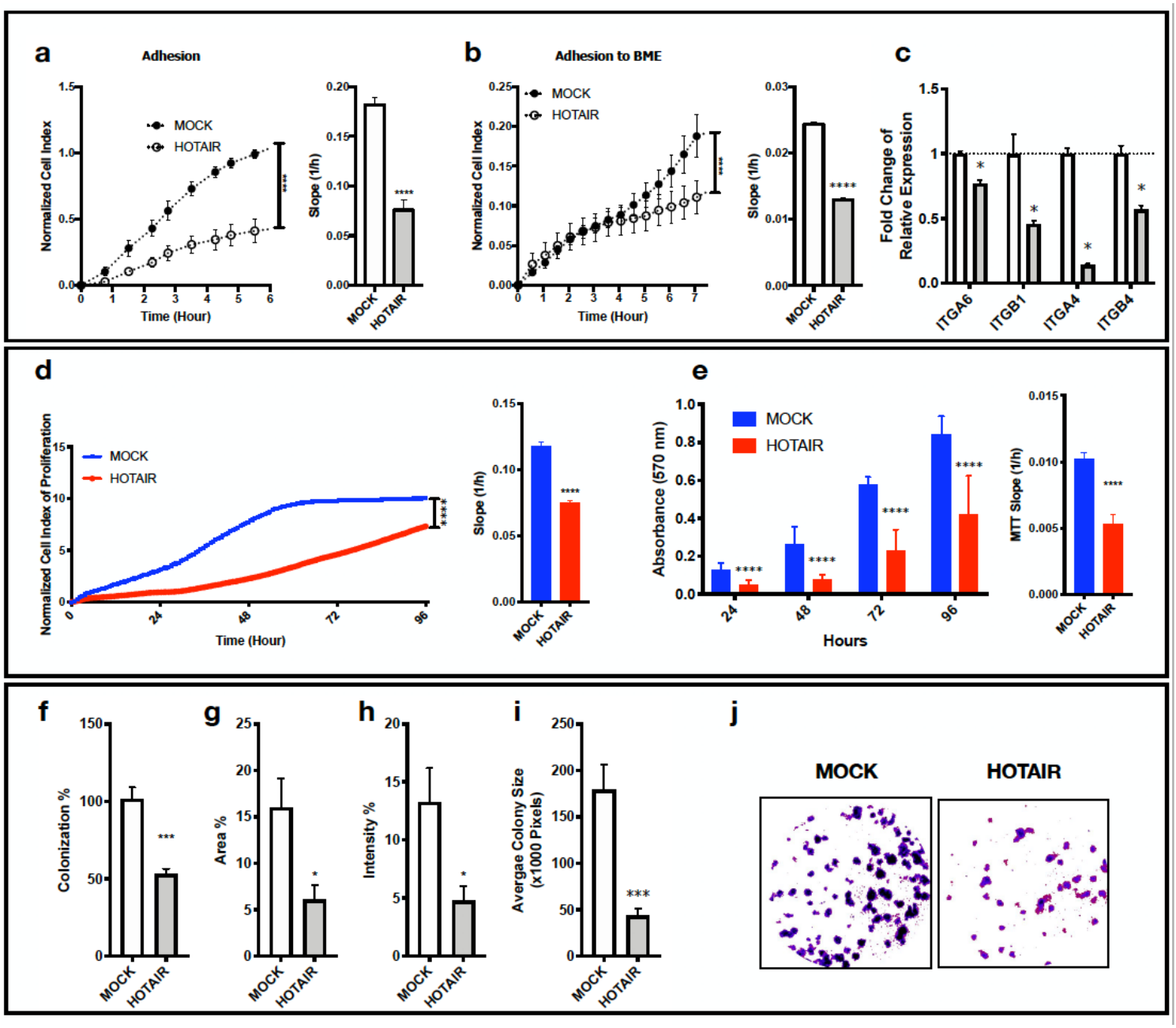

Figure 4

HOTAIR OE induced c-Met inhibition decreases adhesion, proliferation and colony formation Normalized cell index and slope analysis of adhesion to (a) cell culture treated and (b) basal membrane extract-coated surfaces analyzed with xCELLigence RTCA. (c) RT-qPCR analysis of ITGA6, ITGB1, ITGA4 and ITGB4 expressions. (d) Analysis of normalized cell index and rate (slope) of proliferation by xCELLigence RTCA system. Normalized (e) MTT absorbance (570 nm) and proliferation rate (slope) calculated by MTT absorbance. 2D colony formation analysis of MOCK and HOTAIR clones presented as (f) percentage of colonization, (g) percentage of area covered by colonies, (h) intensity of Giemsa-staining (i) average colony size in pixels and (j) representative images of clones generated with ImageJ plugin ColonyArea. 2D colony formation is analyzed by ImageJ plugin ColonyArea. All graphs of experiments are presented as the mean ± SEM of at least 3 independent experiments. * $p \leq 0.05$, ** $p \leq 0.01$, *** $p \leq 0.001$, **** $p \leq 0.0001$.

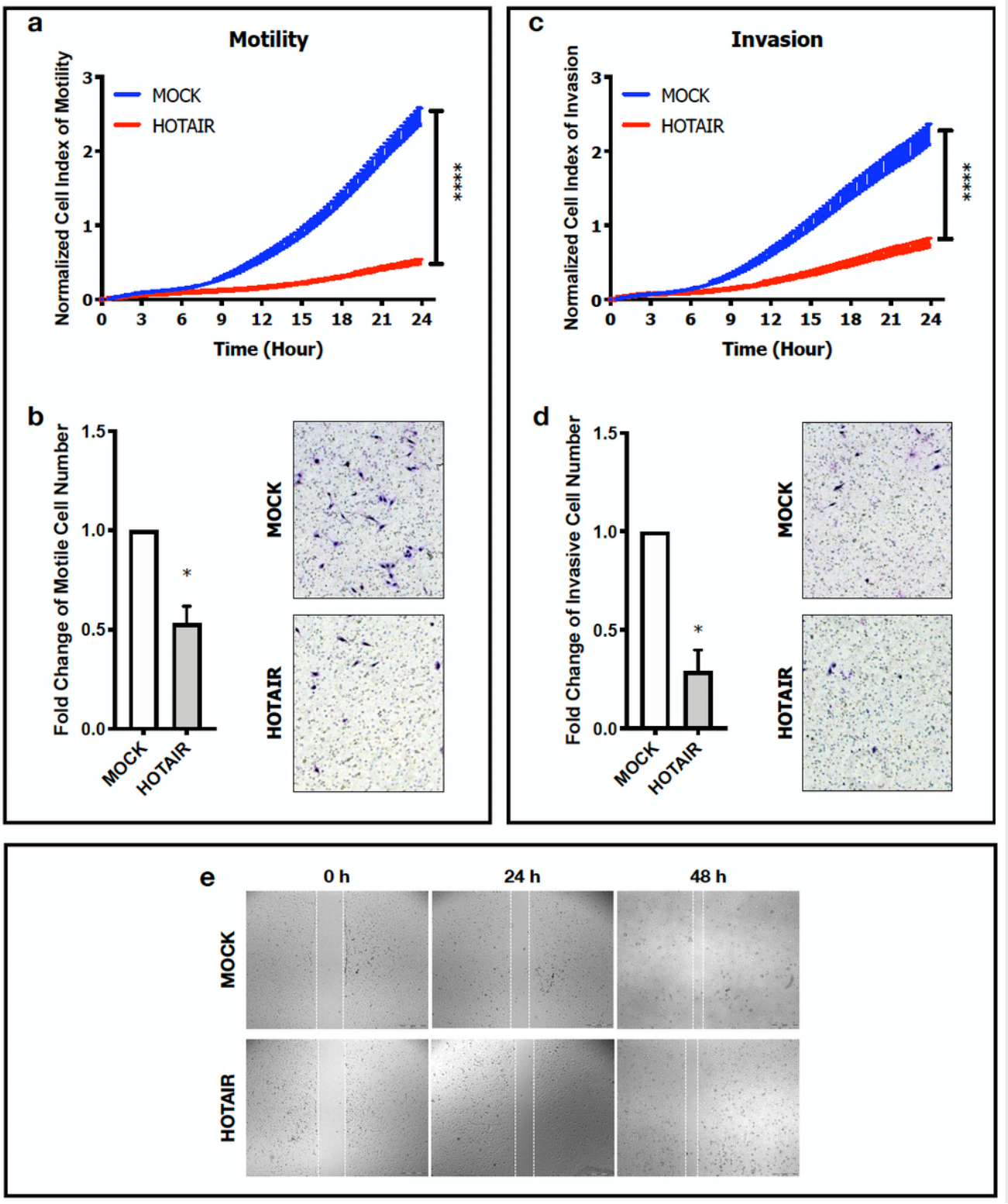

Figure 5

HOTAIR OE induced c-Met inhibition decreases individual motility and invasion ability of SNU-449 cells Real-time (by xCELLigence RTCA) and end-point (cell culture inserts) analysis of motility and invasion of MOCK and HOTAIR OE cell clones. Normalized cell index of (a) motility and (c) invasion analyzed by xCELLigence RTCA system. Fold change graphs and brightfield images of (b) motile and (d) invaded cells in trans-well cell culture inserts. (e) Brightfield microscopy images of 0-, 24- and 48-hour scratch (wound-

healing) assay of MOCK and HOTAIR OE clones. All graphs of experiments are presented as the mean ± SE of at least 3 independent experiments. * p≤ 0.05, **p≤ 0.01, ***p≤ 0.001.

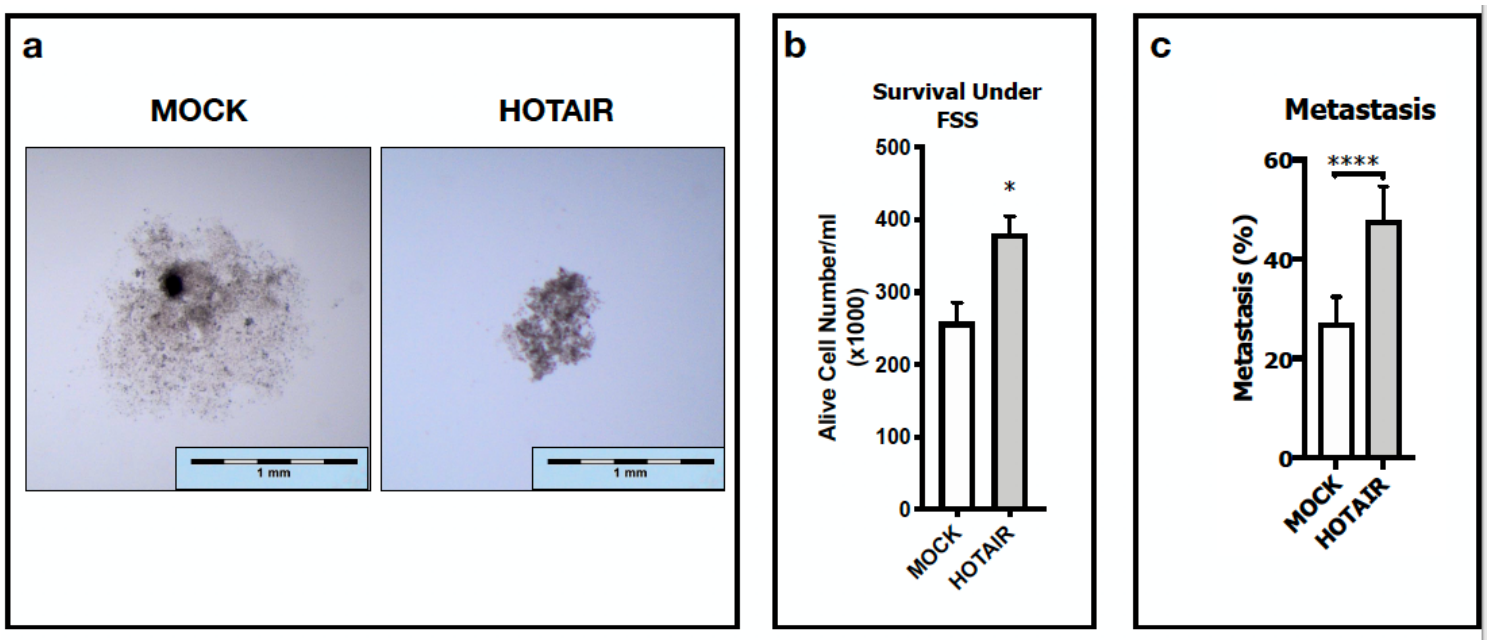

Figure 6

lncRNA HOTAIR suppresses c-Met induced cell scattering, enhances survival under FSS and promotes metastasis in zebrafish embryos Spheroid formation, survival under fluidic shear stress and metastatic capacity of MOCK and HOTAIR OE cells. (a) Spheroid images were collected with stereo-microscopy and magnified equally with scale-bars to generate more clarified presentation of data. (b) Graphical presentation of alive cell numbers of clones cultured under 0.5 dyn/cm2 fluidic shear stress for 1 hour. Embryonic zebrafish xenograft experiments with MOCK and HOTAIR OE SNU-449 cell clones presented as (c) percentage of metastasis in groups that were analyzed in total of four biological experiments. Statistical significance was analyzed by chi-square with Yates correction. All graphs of experiments are presented as the mean ± SE of at least 3 independent experiments. * p≤ 0.05, ** p≤ 0.01, *** p≤ 0.001, **** p≤ 0.0001.

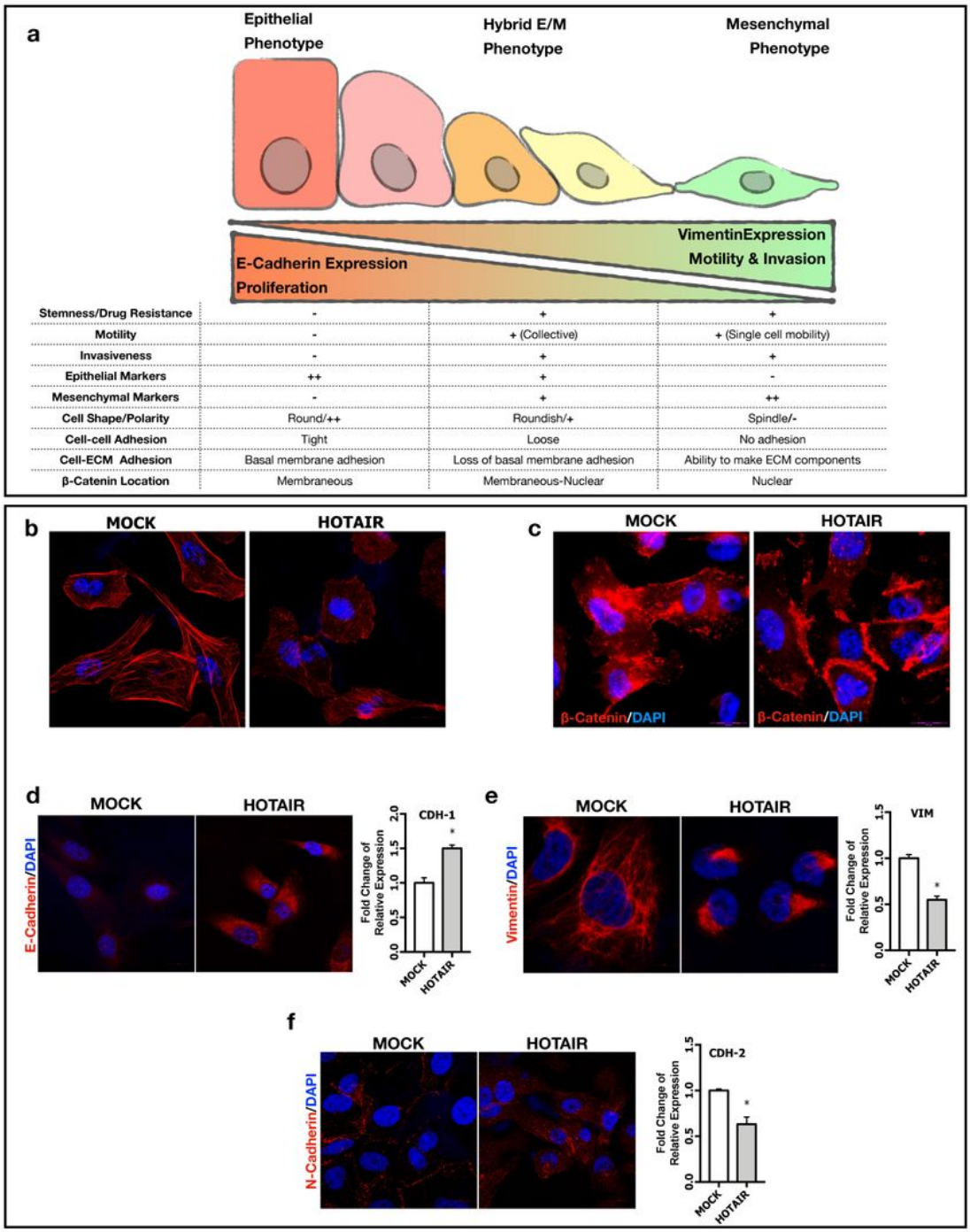

Stemness/Drug Resistance	-	+	+
Motility	-	+ (Collective)	+ (Single cell mobility)
Invasiveness	-	+	+
Epithelial Markers	++	+	-
Mesenchymal Markers	-	+	++
Cell Shape/Polarity	Round/++	Roundish/+	Spindle/-
Cell-cell Adhesion	Tight	Loose	No adhesion
Cell-ECM Adhesion	Basal membrane adhesion	Loss of basal membrane adhesion	Ability to make ECM components
β-Catenin Location	Membraneous	Membraneous-Nuclear	Nuclear

Figure 7

lncRNA HOTAIR maintains hybrid E/M phenotype to promote metastasis (a) Schematic presentation of morphological, molecular and biological biomarkers of epithelial, mesenchymal and hybrid E/M phenotypes. Confocal imaging of (b) Alexa-555 labeled phalloidin staining of F-actin filaments (red). Immunofluorescence imaging of (c) beta-Catenin protein (red) and its cellular localization. Confocal imaging and RT-qPCR analysis of (d) E-Cadherin (e) Vimentin and (f) N-Cadherin expressions. Alexa-594

conjugated secondary antibodies were used in all immunolabeling and confocal imaging experiments. DAPI (blue) was used as nuclear marker in immunofluorescence and confocal images. All graphs of experiments are presented as the mean ± SEM of at least 3 independent experiments. * p≤ 0.05.

Supplementary Files

This is a list of supplementary files associated with this preprint. Click to download.

- TopelSupplementaryFigure2.pdf
- TopelSupplementaryFigure1.pdf
- SupplementaryDocument1.docx